LAWRENCE
LIVERMORE
NATIONAL
LABORATORY

LLNL-TR-843826

Water Mediated Proton Hopping Furazan Mechanism that Accelerates the Decomposition of TATB

B. A. Steele

January 10, 2023

Disclaimer

This work performed under the auspices of the U.S. Department of Energy by Lawrence Livermore National Laboratory under Contract DE-AC52-07NA27344.

Water Mediated Proton Hopping Furazan Mechanism that Accelerates the Decomposition of TATB

Brad A. Steele*

Physical and Life Sciences Division

E-mail: steele26@llnl.gov

Abstract

The dominant initial decomposition mechanism of TATB is believed to be a dehydration reaction that forms mono- and di-furazans, although other mechanisms have been reported. In this work, a mono-furazan mechanism is discovered that involves a proton hopping process between TATB and water. A first principles nudge elastic band calculation was performed that shows the mechanism has an energy barrier of 44.1 kcal/mol, 25.4 kcal/mol lower than the monofurazan mechanism without water. The reaction rate of the proton hopping mechanism was found to be 10^7 to 10^{12} times (at 300-600 K) higher than the mechanism without water. Metadynamics simulations were also performed that indicate the mechanism is qualitatively more probable at lower temperatures (near 300 K) and higher pressures (near 100 bar), although a quantitative confirmation is needed. Future work should focus on modeling the proton hopping mechanism in the condensed state at elevated temperatures (near 600 K).

Introduction

2,4,6-Triamino-1,3,5-trinitrobenzene (TATB, $C_6H_6O_6N_6$) is an insensitive high explosive (HE) that uniquely exhibits two typically contrasting characteristics of being extremely insensitive yet moderately powerful.[1] The insensitivity of TATB is believed to be related to it's layered crystal structure and layer sliding processes that help stabilize the structure under external mechanical stimuli.[2,3] Nevertheless, the sensitivity of HE is inevitably linked to the rate of exothermic decomposition reactions. Understanding the atomistic decomposition mechanisms has been a challenge for TATB. This is partially because there have been many decomposition mechanisms that have been reported[4–15] and the full atomistic pathways, including intermediates, are not well understood.

The energetics and transitions states of the decomposition mechanisms of TATB were modeled from first principles by Wu *et al.*[13] and Tsyshevsky *et al.*[14] using Density Functional Theory (DFT) methods mostly in the gas phase. Wu and Fried calculated the reaction energies for several proposed mechanisms and found that NH_2 scission, ring cleavage, and a single hydrogen release had large reaction energies greater than 100 kcal/mol, while NO_2 scission had a reaction energy of 68.5 kcal/mol. In contrast, the reaction energy for an intra-molecular hydrogen transfer from the amino group to the nitro group was found to be only 35.0 kcal/mol, while the inter-molecular hydrogen transfer had a much higher reaction energy. Wu and Fried proposed two 3 step mechanisms leading to H_2O loss and either a mono-benzofurazan or mono-benzofuroxan-like compound. Note that the mono-benzofurazan-like compound may also be considered a mono-benzofurazan intermediate. The first step was an intra-molecular hydrogen transfer to the biradical (BR) state, and the next step was a rotation of the C-N bond to an intermediate state, then finally a second hydrogen transfer to the final state. Wu and Fried[13] calculated the energy barrier for the first hydrogen transfer to be 47.5 kcal/mol, but did not calculate the energy barrier for the next two steps. Steele calculated the energy barrier to be 69.5 kcal/mol in the gas phase, but found it could potentially be lower in a disordered condensed state.[16] Steele also calculated that

the kinetic isotope effect (KIE) for the furazan mechanism was equal to 1.4 which matches experiment. This adds support in favor of this mechanism. Tsyshevsky *et al.* modeled a different mechanism for H_2O loss and a furazan derivative as two sequential hydrogen transfers with a barrier of 65.3 kcal/mol.[14] Tsyshevsky *et al.* also modeled the CONO mechanism and the HONO release mechanism and found that the CONO mechanism had the smallest barrier of 54.9 kcal/mol. However, Tsyshevsky also found the NO_2 scission mechanism had a large prefactor (10^{18} s^{-1}) in the reaction rate, which made the NO_2 scission mechanism favorable at high temperatures.[14]

Molecular dynamics (MD) simulations are instructive for understanding the decomposition chemistry and to quantify the kinetics for decomposition. Several high temperature (2000 K+) MD simulations have noted that NO_2 scission is a dominant initial step of decomposition of TATB using Reax force fields and Density Functional Tight Binding (DFTB) methods.[17–22] Intra-molecular hydrogen transfer and water, hydroxyl (OH), and NO release mechanisms have also been suggested from these studies.[18–21] Mono- and dibenzofurazans accompanied by water were reported in the shock simulations by Manaa *et al.* using DFTB.[11] Manaa *et al.* also reported the formation of nitrogen-rich heterocycles that inhibits the formation of the final decomposition products N_2 and solid carbon and therefore inhibits exothermic chemistry.[11] Decomposition mechanisms that produce N_2 under shock compression have been suggested by Tiwari *et al.*.[19]

The consensus from these studies and others[23] has been that the dehydration reaction leading to furazans and reactions leading to furoxans are the dominant initial decomposition mechanisms of TATB, however there have been reports of many other mechanisms. In this work, we wish to gain a better understanding of the the decomposition mechanisms of TATB by modeling decomposition mechanisms of TATB in the presence of water. In order to describe the strength of chemical bonds most accurately we used using Density Functional Theory (DFT). We performed Nudged Elastic Band (NEB) calculations to obtain the transition state of a furazan mechanism in the presence of water. Metadynamics simulations

were performed to model the the decomposition mechanisms and to qualitatively model the pressure and temperature effects on those mechanisms.

Computational Methods

General DFT Parameters

To model the component decomposition mechanisms of TATB the energetics and kinetic rates of 7 mechanism were modeled. The energetics along the reaction coordinates were modeled by performing a combination of geometry optimizations, nudged elastic band (NEB), and thermodynamic integration (TI) simulations with a single TATB molecule using the CP2K simulation package at the DFT level.[24] The forces were obtained via QuickStep's implementation of DFT with the GPW approach.[25–29] GPW is a dual basis set method utilizing both Gaussian type orbital basis set (TZV2P) and plane-waves expanded to 400 Rydberg cutoff for the valence electronic density. Norm conserving GTH pseudopotentials were utilized for the core electronic states.[30,31] PBE exchange-correlation functional with Grimme dispersion correction was utilized due to its predictability and computational efficiency.[32,33] The energy tolerance for SCF cycles was set to 1×10^{-7} hartree.

NEB Parameters

Geometry optimizations were performed for local minima along the reaction coordinates, *i.e.* the initial, intermediate, and final states. The positions of the atoms were optimized until the forces were less than 1×10^{-3} Hartree/bohr and the maximum displacement between optimization steps was less than 5×10^{-3} Å. Climbing image nudge elastic band (CI-NEB)[34,35] calculations were performed to obtain transition state molecular structures and energies. The number of replicas in the CI-NEB were chosen so that the distance between any two replicas were less than 2 Å to prevent abrupt changes in the structure or energy. Force constants between each adjacent bead was set to 560.3 kcal/mol $\cdot$ Å^{-2}. Calculations were

performed until the maximum displacement, root mean square displacement, and maximum force converged to less than 5×10^{-3} Å, 2.5×10^{-3} Å, and 1.1 kcal/mol $\cdot$ Å^{-1} respectively were met on each atom.

Metadynamics Parameters

Metadyanmics[36] simulations were performed using 2 TATB molecules with and without 3 H_2O molecules. Two collective variables (S1 and S2) were chosen to accelerate the reaction that produces a monofurazan. However, other mechanisms are also accelerated with these collective variables (CVs). The CVs are defined to be related to the coordination number, which is approximately equal to 1 when two atoms are covalently bonded and equal to 0 when they are not. The functional form of the coordination number is:

$$S(r) = \frac{1 - (r/R_0)^{NN}}{1 - (r/R_0)^{ND}} \tag{1}$$

The first CV, S1, is chosen to be the coordination between nitrogen and oxygen atoms. The second CV, S2, was chosen to be the coordination between oxygen and hydrogen atoms. S1 was chosen to accelerate cleavage of the nitrogen-oxygen bond in the nitro group of TATB and S2 was chosen to accelerate hydrogen transfer processes to oxygen atoms on the nitro group of TATB and water molecules. For S1, values of 10, 18, and 1.59 Å were used and for S2, values of 10, 16, and 1.16 Å were used for NN, ND, and R_0 respectively. Repulsive potential was laid down every 7.5 fs with a height of 3.13 kcal/mol.

Results and discussion

A proton-hopping (PHOP) decomposition mechanism of TATB mixed with 3 H_2O molecules was discovered that creates a monofurazan intermediate and water. The energy barrier for this mechanism is much lower than the barrier without water in the gas phase.[13,16] The activation energy barriers that were calculated with/without water using the NEB method

Table 1: Calculated activation energies (E_A) and Zero-Point Energies (ZPE) at 0 K for the furazan decomposition mechanisms of TATB.

H_2O Molecules	**E_A (kcal/mol)**	**ZPE (kcal/mol)**
0	69.5	5.3
3	44.1	4.6

are given in Table 1. The barrier was calculated to be 69.5 kcal/mol without water and 44.1 kcal/mol with the PHOP mechanism with 3 H_2O molecules. The presence of water lowers the barrier by 25.4 kcal/mol, which is a large decrease.

The PHOP mechanism involves proton-hopping from the amino group of TATB through 2 H_2O molecules while a 3rd water molecule makes a hydrogen bond with the water and the amino group of TATB. The NEB method optimizes the pathway such that it is the minimum energy pathway (MEP) from one local minima to another. The energy along the MEP for each bead in the NEB calculation is displayed in Fig. 1 and the corresponding image of the molecular structure at each bead is displayed in Fig. 2. The hydrogen from the amino group of TATB is transferred to the first water molecule, then a hydrogen from the first water molecule is transferred to the second water, see bead 9 in Fig. 2. The second water molecule then transfers a hydrogen to the nitro group (bead 11), followed by an intra-molecular hydrogen transfer from the amino group to the nitro group which releases a water (bead 13). Bead 13 is the transition state. The mechanism makes monobenzofurazan tautomer. It is a tautomer because the hydrogen is located on the 5-membered furazan ring.

The reaction rate for the PHOP mechanism was calculated by performing a vibrational calculation at the transition state (bead 13) and using the energy barrier calculated with the NEB method and assuming an arrhenius rate law,[37] displayed in Fig. 3. The rate of the PHOP mechanism is compared to the rate calculated without water in ref.[16] Also to get a rough estimate of the timescales involved in the reaction 1/hour and 1/(10 years) is also displayed. The reaction rate of the PHOP mechanism is calculated to be 7-12 orders of magnitude higher than the monobenzofurazan mechanism that involves intra-molecular

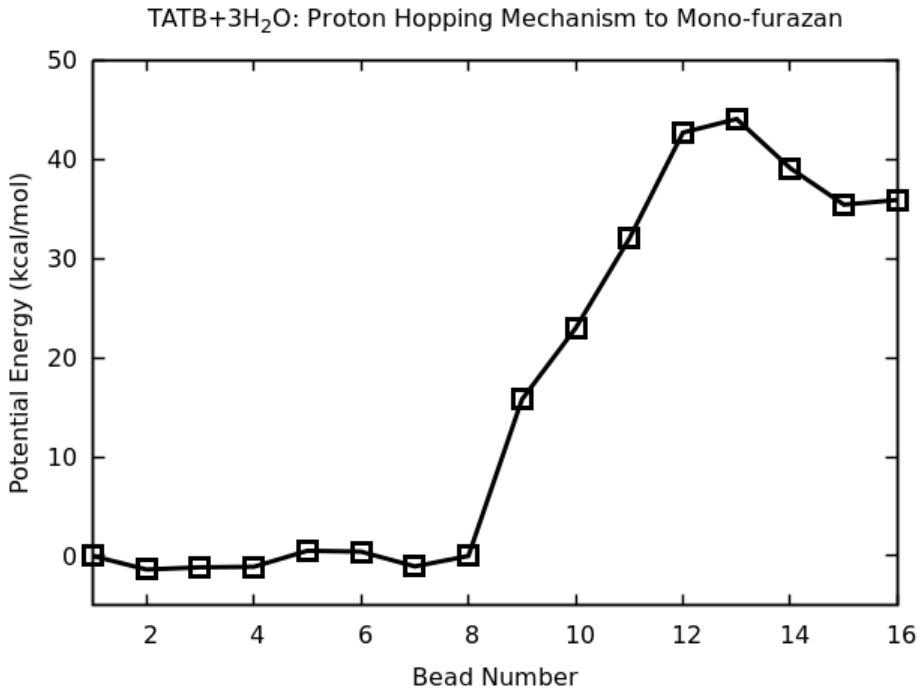

Figure 1: Energy profile for the proton-hopping furazan decomposition mechanism calculated using the NEB method. The x-axis is the bead number in the NEB calculation. Snapshots of some beads are displayed in Figure 2.

hydrogen transfer. The vibrational calculation also confirms that bead 13 is the transition state because there is 1 and only 1 imaginary frequency.

Metadyanmics simulations were also performed to explore various reaction pathways focused on the hydrogen transfer mechanisms leading to monofurazan. The initial simulation cell that was in the metadynamics simulation is displayed in Fig. 4, which consists of 2 TATB molecules and 3 water molecules in a 20x20x20 $Å^3$ box. The simulation box is large to avoid self-interaction. Two TATB molecules were used to potentially model inter-molecular hydrogen transfer processes. The two TATB molecules were initially arranged in the same layer so that the inter-molecular distance between the oxygen and hydrogen atoms were small. The system was thermalized at 300 K for about 5 ps with fixed number of atoms, volume of the cell, and temperature (NVT). The simulation box is large, so the pressure at 300 K was -68 bar. Since the pressure is negative, the simulation with the large cell is only qualitatively representative of a low pressure system. An additional set of metadynamics

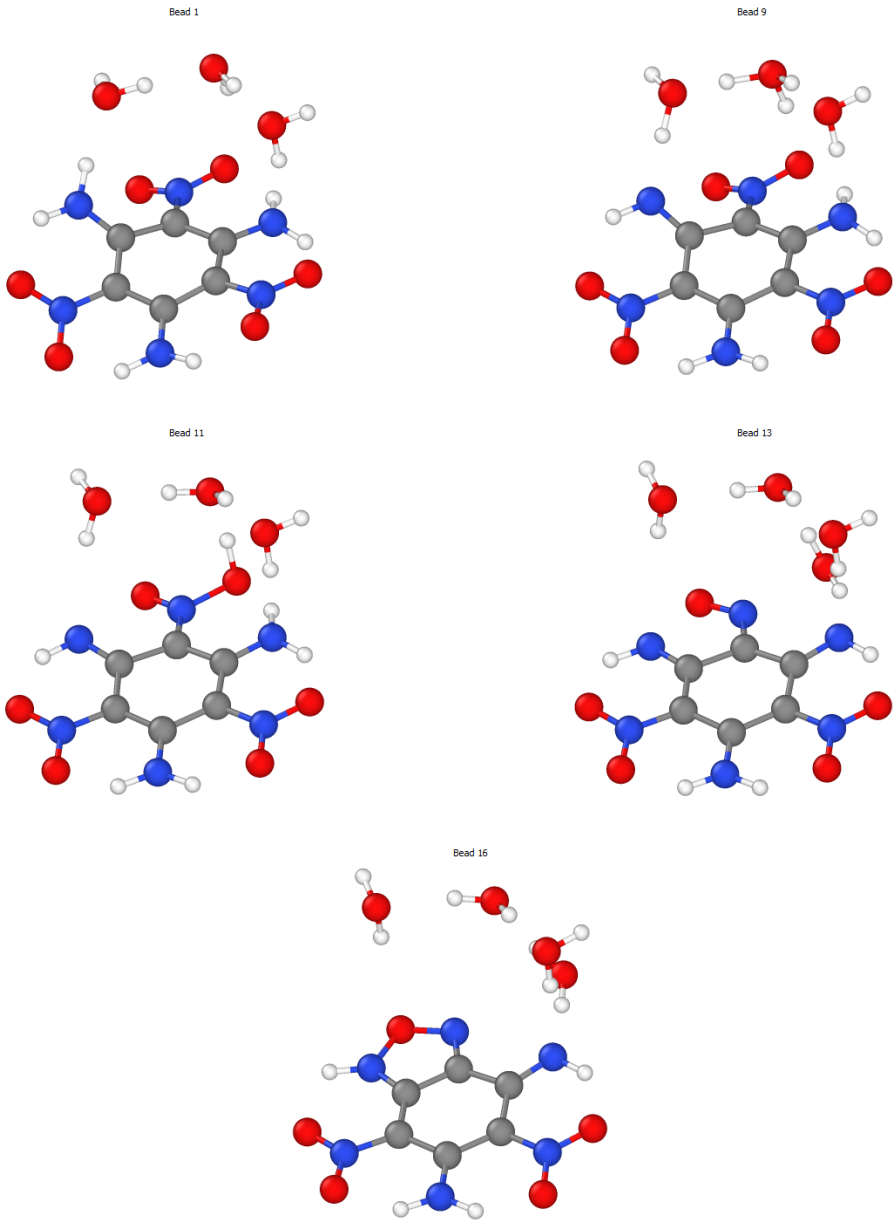

Figure 2: Snapshots of the molecular structure of the proton-hopping furazan mechanism modeld with the NEB method. The bead number in the NEB calculation is displayed corresponding to the bead number in Fig. 1.

simulations were performed at a fixed pressure of 100 bar, to qualitatively represent a higher pressure result.

Snapshots of the molecular structure during the metadynamics simulation at 300 K is displayed in Fig. 5. There are several intra-molecular hydrogen transfers such as the ones

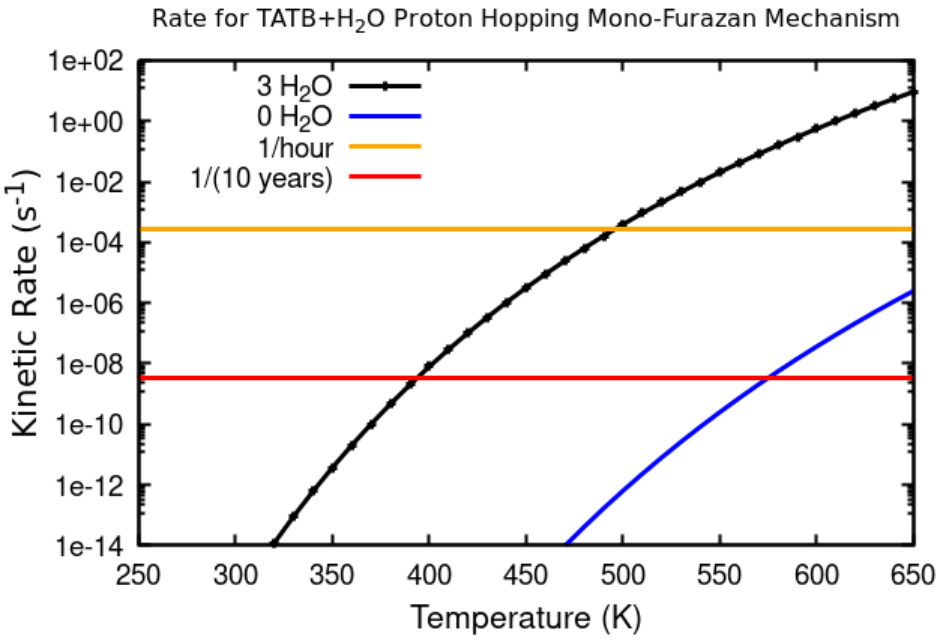

Figure 3: The calculated reaction rate vs temperature for the proton-hopping mechanisn with 3 H_2O molecules and the mechanism without water calculated in ref.[16]

displayed at 8.17 meta ps and 13.24 meta ps. At 13.82 meta ps, the proton-hopping process occurs to transfer a hydrogen from the amino group to the nitro group nearly simultaneously as an intra-molecular hydrogen transfer occurs which releases a water and makes the monofurazan tautomer. This mechanism is very similar to the one modeled with the NEB method. A second proton-hopping process occurs that transfers a hydrogen to the amino group to create the monobenzofurazan displayed at 23.75 meta ps. At a later time in the simulation, instead of making a difurazan, there was instead a ring opening process displayed at 30.78 meta ps. The ring opening occured via an intra-molecular hydrogen transfer and a hydrogen transfer to the water. It is possible that this second ring opening mechanism is an artifact of overdriving the reaction in the metadynamics. Nevertheless, the metadynamics simulation does show a similar mechanism as the one modeled with the NEB method which is additional confirmation that this mechanism is a highly probably mechanism with TATB mixed with water. It is not clear exactly what the ratio of water to TATB is necessary

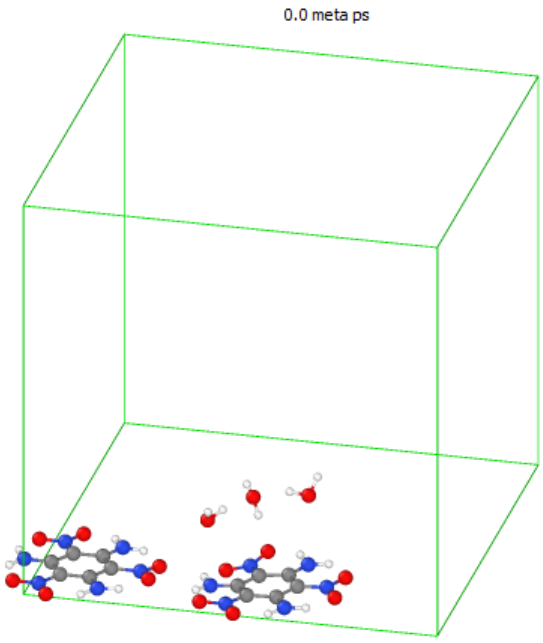

Figure 4: Snapshots of the initial structure used in the metadynamics simulations that consists of 2 TATB molecules and 3 water molecules. The simulation box is 20x20x20 $Å^3$ to avoid self-interaction.

for this reaction to be significant, since this was not studied, but the results qualitatively indicates that the decomposition of TATB can be significantly accelerated in the presence of water.

Another metdynamics simulation at 300 K was also performed without water and no reaction was oberved after 31 ps. This is additional evidence that water accelerates the monofurazan mechanism significantly.

Another aspect of the PHOP mechanism to consider are entropic effects because the energy barrier calculated with the NEB method does not include entropy in the energy barrier. It is plausible that the PHOP mechanism may not be entropically favorable because it requires 2 or 3 water molecules and a TATB molecule to collide with each other in a particular geometry in order for the mechanism to be possible. The required geometry is one of many macrostates that are thermodynamically accessible and so therefore the reaction may not be entropically favorable.

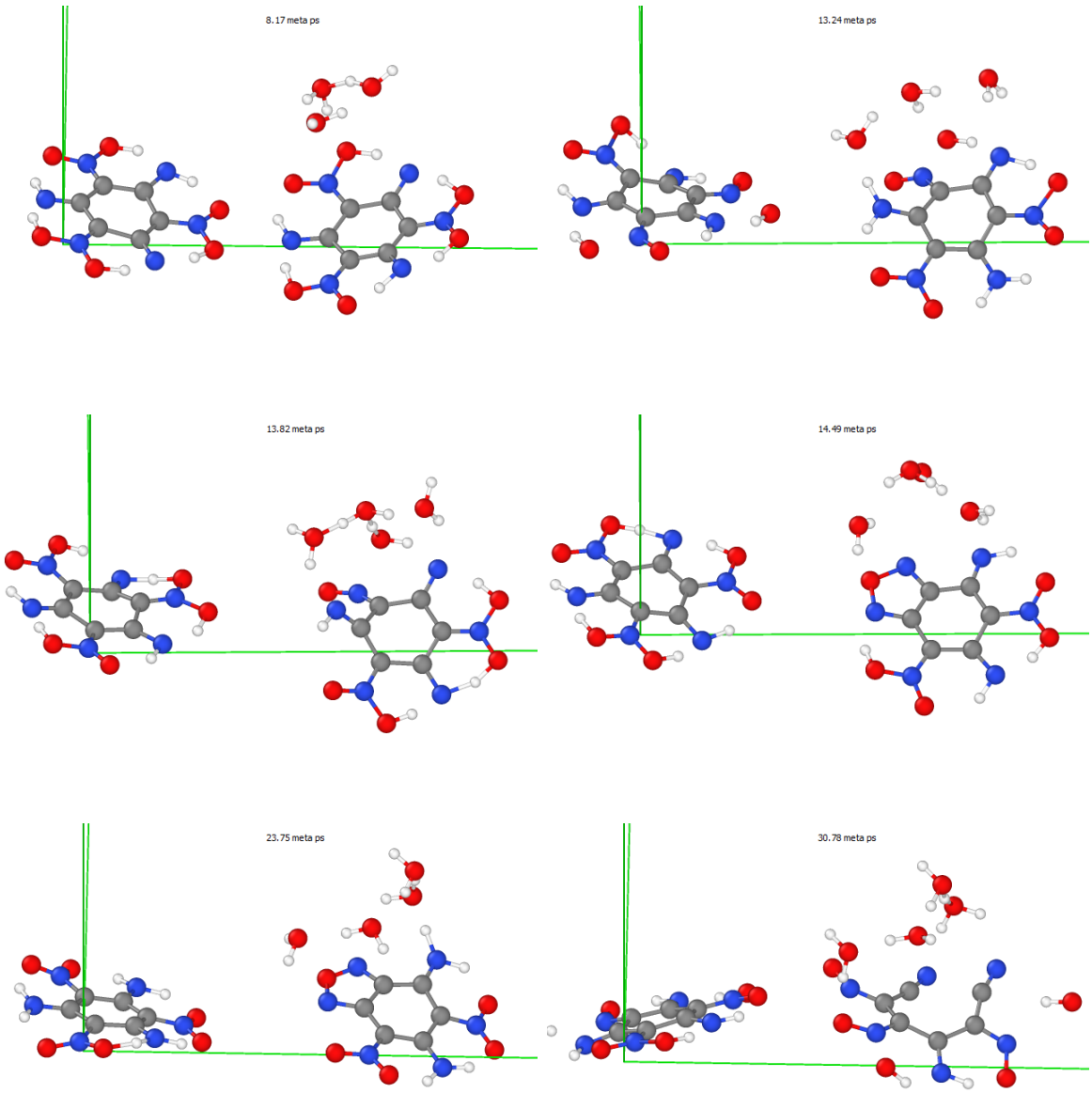

Figure 5: Snapshots of the molecular structure of the proton-hopping monofurazan mechanism modeled with metadynamics at 300 K at low pressure. The timestamp in the metadynamics simulation is displayed in each image. The monofurazan is displayed at 23.75 meta ps. At a later time, ring opening mechanism occurs displayed at timestamp 30.78 meta ps.

In an attempt to test whether the PHOP mechanism is entropically unfavorable another metadynamics simulation was performed at 600 K, snapshots of the structure are displayed in Fig. 6. Interestingly the PHOP mechanism did not occur. Instead intra- and inter-molecular

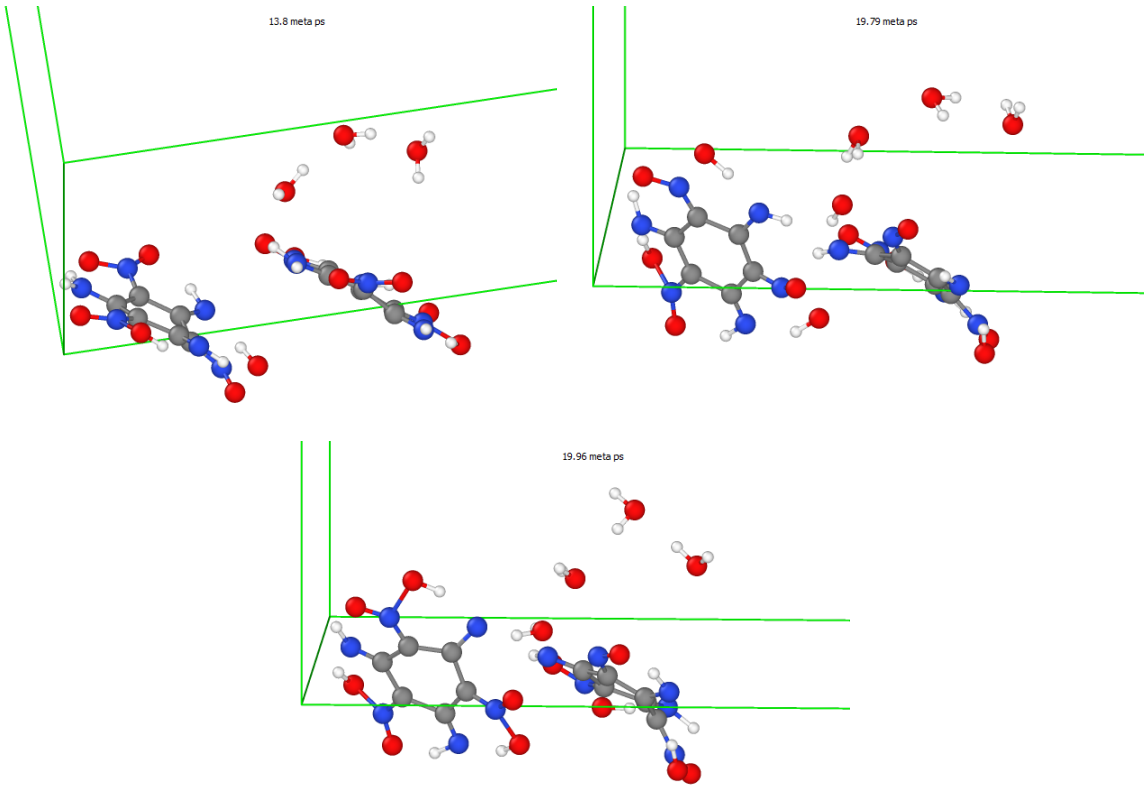

Figure 6: Snapshots of the molecular structure in the metadynamics simulation at 600 K at low pressure. The monofurazan mechanism does not occur, instead a combination of an intra- and inter- molecular hydrogen transfer lead to water release.

hydrogen transfer processes occured that released a water. Inter-molecular hydrogen transfer has been found to have a higher barrier than intra-molecular hydrogen transfer by Wu *et al.* without water present.[13] Since the PHOP mechanism was not observed 600 K, but did occur at 300 K it is plausible that the mechanism is not entropically favorable. It is also possible that this may an issue assosciated with thermodynamic sampling.

Higher pressures may increase the probability of the PHOP mechanism because it reduces the overall volume and therefore increases the probability that the molecules will collide. The original system was thermalized at 300 K at 100 bar for 20 ps, then at 600 K and 100 bar for another 15 ps. The system transformed into a condensed state with water mixed into the structure displayed in Fig. 7. A more appropriate system for the simulation would be

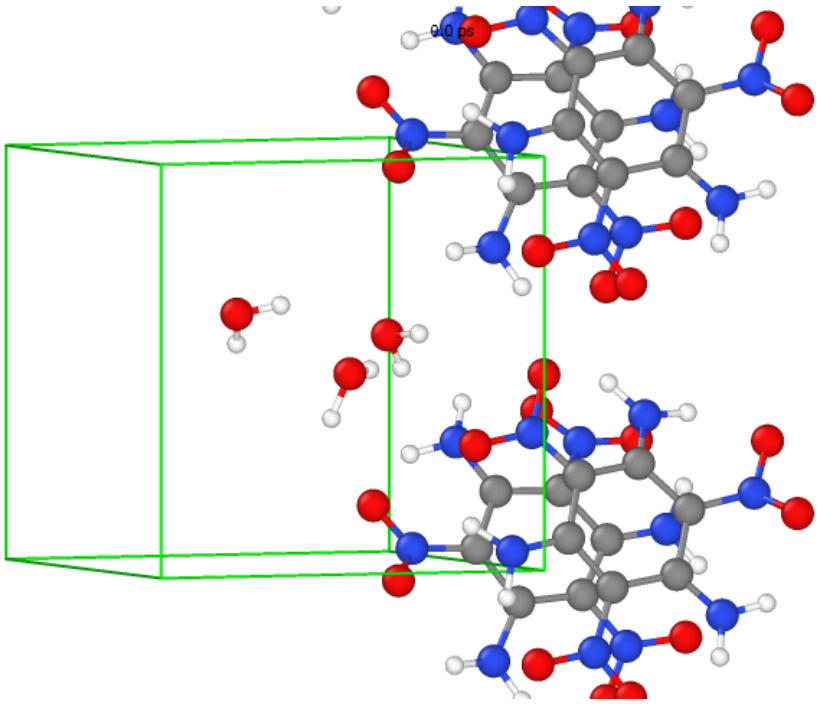

Figure 7: Snapshots of the initial structure in the metadynamics simulations that consists of 2 TATB molecules and 3 water molecules at 600 K and a pressure of 100 bar. Some periodic images are displayed to show that the structure is partially layered with water mixed into the structure.

to simulate a surface of TATB arranged in the crystal structure which would require more atoms in the simulation. Here the system size is kept small for computational efficiency, but there are likely self interaction issues for such a small system size. Nevertheless, this small system can still qualiatively represent the effect pressure can have on the PHOP mechanism.

The PHOP mechanism does occur at 600 K at 100 bar, displayed in Fig. 8. The mechanism only involves 1 water molecule while the other two water molecules make hydrogen bonds. The mechanism involves an intra-molecular hydrogen transfer and an inter-molecular hydrogen transfer mediated through the water. Since the PHOP mechanism does occur at 100 bar, but not at a low pressure at 600 K we conclude that pressure qualitatively makes the PHOP mechanism more probably to occur. This is likely due to entropic effect that increases the probability of molecular collisions, and although the simulation cell is too small to make strong conclusions this qualitative effect should still have an impact in larger simulation cells.

At a later time in the metadynamics simulation at 600 K and 100 bar there is a ring-

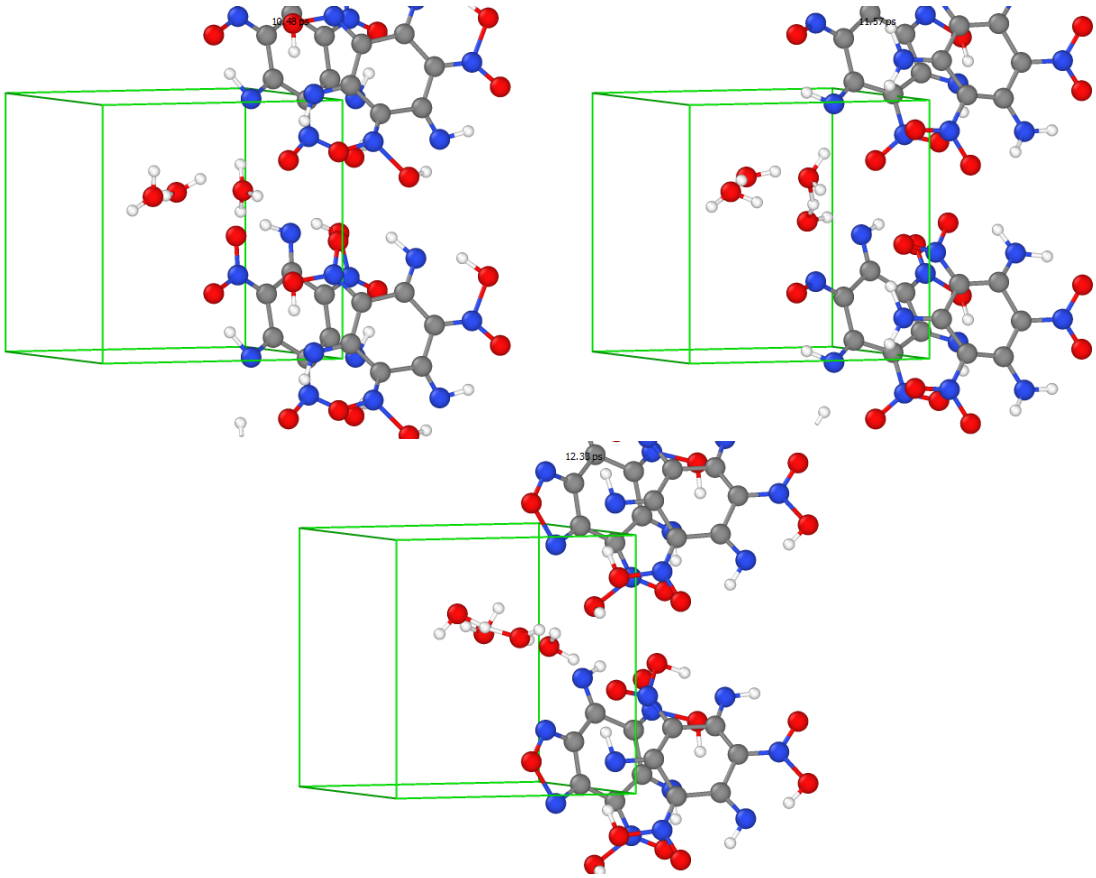

Figure 8: Snapshots of the molecular structure of the proton-hopping monofurazan mechanism modeled with metadynamics at 600 K at a pressure of 100 bar. The timestamp in the metadynamics simulation is displayed in each image. The monofurazan is displayed in the bottom image at 12.38 meta ps.

cleavage mechanism that occurs via hydrogen transfer OH transfer processes, displayed in Fig. 9. After the OH transfer, the ring opens as shown at 16.38 meta ps. This quickly leads to ring cleavage at 16.75 meta ps. This mechanism may be related to the ring cleavage mechanism reported by Ostmark.[9]

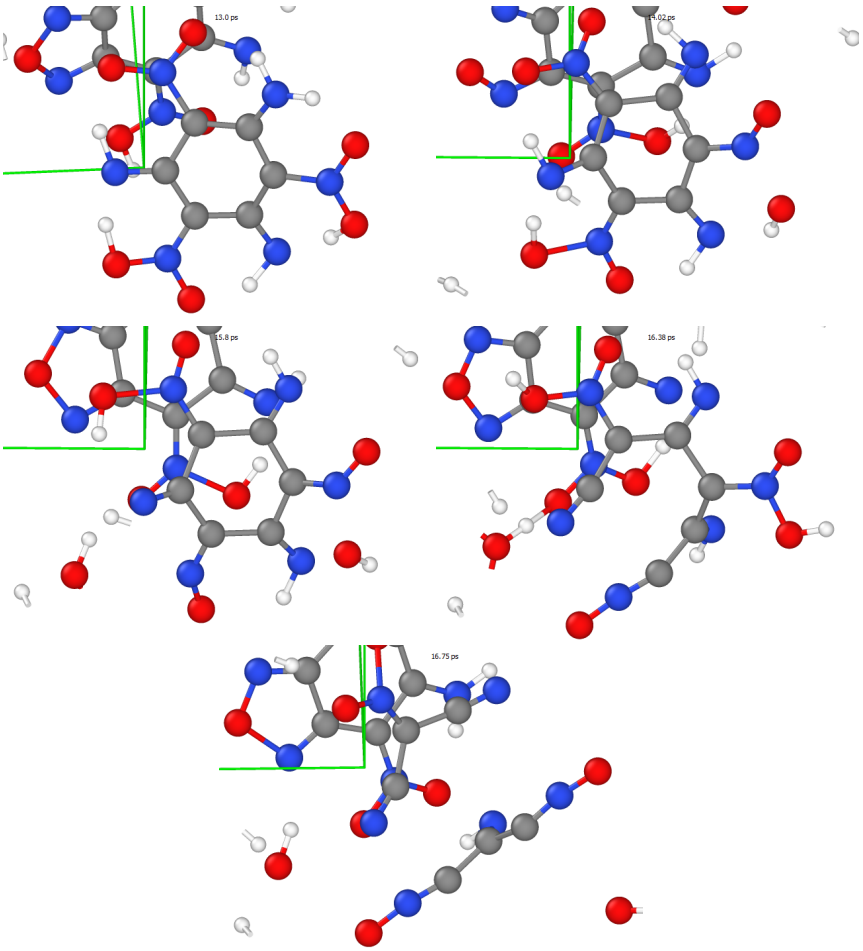

Figure 9: Snapshots of the molecular structure of a ring-cleavage mechanism modeled with metadynamics at 600 K at a pressure of 100 bar. The timestamp in the metadynamics simulation is displayed in each image.

Conclusions

Ab initio modeling methods were used to discover a proton hopping mechanism between TATB and water that lowers the energy barrier of the monofurazan mechanism by 25.4 kcal/mol and increases the rate of decomposition by 7-12 orders of magnitude. The energy barrier and transition state were found using the NEB method. A vibrational calculation assuming harmonic vibrational modes was performed at the transition state to confirm the transition state has one and only one imaginary mode. The mechanism was also observed in a metadynamics simulation at 300 K at low pressure, but a different mechanism occured at 600 K. This qualitatively indicates that the mechanism is not entropically favorable and is

less likely to occur at higher temperatures. However, a similar proton-hopping mechanism was also observed at 600 K at a pressure of 100 bar which qualitatively indicates that pressure increases the probability of the proton hopping mechanism. The simulation cell at 100 bar was too small to make quantitative conclusions. Future work should focus on quantifying the barrier and reaction rate of the proton hopping mechanism in the condensed state as a function of pressure and temperature. This work demonstrates that the proton hopping mechanism with TATB and water exists and that it can lower the barrier by a large amount, but we can only provide qualitative evidence that the mechanism may or may not be possible at elevated temperatures where the decomposition of TATB is observed experimentally.

Acknowledgement

This work was performed under the auspices of Lawrence Livermore National Laboratory operated by Lawrence Livermore National Security, LLC, for the U.S. Department of Energy, National Nuclear Security Administration under Contract DE-AC52-07NA27344. Funding was provided by the National Nuclear Security Administration, Directed Stockpile Work (DSW) and by Lawrence Livermore National Laboratory, WCI Weapon Technologies and Engineering Program. Special thanks to Alan Burnham, John Reynolds, Keith Coffee, Batikan Koroglu, I-Feng Kuo, and Jason Moore for illuminating discussions. The manuscript has been approved for unlimited release under release number LLNL-JRNL-XXXXX.

References

(1) Dobratz, B. M. The insensitive high explosive triaminotrinitrobenzene (TATB): Development and characterization, 1888 to 1994. **1995**,

(2) Zhang, C.; Wang, X.; Huang, H. π-stacked interactions in explosive crystals: buffers

against external mechanical stimuli. *Journal of the American Chemical Society* **2008**, *130*, 8359–8365.

(3) Bu, R.; Xiong, Y.; Zhang, C. π–π Stacking Contributing to the Low or Reduced Impact Sensitivity of Energetic Materials. *Crystal Growth & Design* **2020**, *20*, 2824–2841.

(4) Farber, M.; Srivastava, R. Thermal decomposition of 1,3,5-triamino-2,4,6-trinitrobenzene. *Combustion and Flame* **1981**, *42*, 165–171.

(5) Sharma, J.; Garrett, W.; Owens, F.; Vogel, V. X-ray photoelectron study of electronic structure, ultraviolet, and isothermal decomposition of 1, 3, 5-triamino-2, 4, 6-trinitrobenzene. *The Journal of Physical Chemistry* **1982**, *86*, 1657–1661.

(6) Sharma, J.; Forbes, J.; Coffey, C.; Liddiard, T. The physical and chemical nature of sensitization centers left from hot spots caused in triaminotrinitrobenzene by shock or impact. *Journal of Physical Chemistry* **1987**, *91*, 5139–5144.

(7) Land, T. A.; Siekhaus, W. J.; Foltz, M. F.; Behrens, R. J. Condensed-phase thermal decomposition of TATB investigated by atomic force microscopy (AFM) and simultaneous thermogravimetric modulated beam mass spectrometry (STMBMS). *10th International Det Symposium* **1993**,

(8) Makashir, P.; Kurian, E. Spectroscopic and thermal studies on the decomposition of l, 3, 5-triamino-2, 4, 6-trinitrobenzene (TATB). *Journal of thermal analysis* **1996**, *46*, 225–236.

(9) Östmark, H. Shock induced sub-detonation chemical reactions in 1, 3, 5-triamino-2, 4, 6-trinitrobenzene. *AIP Conference Proceedings* **1996**, *370*, 871–874.

(10) Belmas, R.; Bry, A.; David, C.; Gautier, L.; Keromnes, A.; Poullain, D.; Thevenot, G.; Gallic, C.; Chenault, J.; Guillaumet, G. Preheating Sensitization of a TATB Compo-

sition Part one: Chemical Evolution. *Propellants, Explosives, Pyrotechnics* **2004**, *29*, 282–286.

(11) Manaa, M. R.; Reed, E. J.; Fried, L. E.; Goldman, N. Nitrogen-rich heterocycles as reactivity retardants in shocked insensitive explosives. *Journal of the American Chemical Society* **2009**, *131*, 5483–5487.

(12) Fried, L.; Najjar, F.; Howard, W. M.; Manaa, M. R.; Bastea, S. Multiscale simulation of hot spot ignition. APS Shock Compression of Condensed Matter Meeting Abstracts. 2011; pp CKT–20.

(13) Wu, C. J.; Fried, L. E. Ring Closure Mediated by Intramolecular Hydrogen Transfer in the Decomposition of a Push-Pull Nitroaromatic: TATB. *The Journal of Physical Chemistry A* **2000**, *104*, 6447–6452.

(14) Tsyshevsky, R. V.; Sharia, O.; Kuklja, M. M. Molecular Theory of Detonation Initiation: Insight from First Principles Modeling of the Decomposition Mechanisms of Organic Nitro Energetic Materials. *Molecules* **2016**, *21*.

(15) Moore, J. S.; McClelland, M. A.; P.C., H.; Kahl, E. *Modeling of Thermal Decomposition of TATB-Based Explosive for Safety Analysis*; WCI Report-CODT-2020-0439, 2020.

(16) Steele, B. A. Initial Decomposition Mechanisms of 2,4,6-triamino-1,3,5-trinitrobenzene (TATB) and their Kinetic Isotope Effect. *To be published* **2022**,

(17) Zhang, L.; Zybin, S. V.; Van Duin, A. C.; Dasgupta, S.; Goddard III, W. A.; Kober, E. M. Carbon cluster formation during thermal decomposition of octahydro-1, 3, 5, 7-tetranitro-1, 3, 5, 7-tetrazocine and 1, 3, 5-triamino-2, 4, 6-trinitrobenzene high explosives from ReaxFF reactive molecular dynamics simulations. *The Journal of Physical Chemistry A* **2009**, *113*, 10619–10640.

(18) Wen, Y.; Xue, X.; Long, X.; Zhang, C. Cluster Evolution at Early Stages of 1,3,5-Triamino-2,4,6-trinitrobenzene under Various Heating Conditions: A Molecular Reactive Force Field Study. *The Journal of Physical Chemistry A* **2016**, *120*, 3929–3937, PMID: 27182789.

(19) Tiwari, S. C.; Nomura, K.-i.; Kalia, R. K.; Nakano, A.; Vashishta, P. Multiple reaction pathways in shocked 2, 4, 6-triamino-1, 3, 5-trinitrobenzene crystal. *The Journal of Physical Chemistry C* **2017**, *121*, 16029–16034.

(20) He, Z.-H.; Yu, Y.; Huang, Y.-Y.; Chen, J.; Wu, Q. Reaction kinetic properties of 1, 3, 5-triamino-2, 4, 6-trinitrobenzene: A DFTB study of thermal decomposition. *New Journal of Chemistry* **2019**, *43*, 18027–18033.

(21) Huang, X.; Zhao, X.; Long, X.; Dai, X.; Zhang, K.; Li, M.; Guo, F.; Qiao, Z.; Wen, Y. Comparison study of carbon clusters formation during thermal decomposition of 1, 3, 5-triamino-2, 4, 6-trinitrobenzene and benzotrifuroxan: a ReaxFF based sequential molecular dynamics simulation. *Physical Chemistry Chemical Physics* **2020**, *22*, 5154–5162.

(22) Kroonblawd, M. P.; Fried, L. E. High explosive ignition through chemically activated nanoscale shear bands. *Phys. Rev. Lett.* **2020**, *124*, 206002.

(23) Coffee, K. R.; Panasci-Nott, A. F.; Stewart, B. J.; Olivas, J. A.; Williams, A. M.; Reynolds, J. G. Trace Compound Analysis in TATB by Liquid Chromatography coupled with Spectroscopic and Spectrometric Detection. *Propellants, Explosives, Pyrotechnics* **2022**, *47*, e202100224.

(24) Hutter, J.; Iannuzzi, M.; Schiffmann, F.; VandeVondele, J. cp2k: atomistic simulations of condensed matter systems. *WIREs Computational Molecular Science* **2014**, *4*, 15–25.

(25) Hohenberg, P.; Kohn, W. Inhomogeneous Electron Gas. *Phys. Rev.* **1964**, *136*, B864–B871.

(26) Kohn, W.; Sham, L. J. Self-Consistent Equations Including Exchange and Correlation Effects. *Phys. Rev.* **1965**, *140*, A1133–A1138.

(27) Lippert, G.; Hutter, J.; Parrinello, M. A hybrid Gaussian and plane wave density functional scheme. *Molecular Physics* **1997**, *92*, 477–488.

(28) VandeVondele, J.; Krack, M.; Mohamed, F.; Parrinello, M.; Chassaing, T.; Hutter, J. Quickstep: Fast and accurate density functional calculations using a mixed Gaussian and plane waves approach. *Comput. Phys. Commun.* **2005**, *167*, 103–128.

(29) VandeVondele, J.; Borštnik, U.; Hutter, J. Linear Scaling Self-Consistent Field Calculations with Millions of Atoms in the Condensed Phase. *J. Chem. Theory Comput.* **2012**, *8*, 3565–3573.

(30) Goedecker, S.; Teter, M.; Hutter, J. Separable dual-space Gaussian pseudopotentials. *Phys. Rev. B* **1996**, *54*, 1703–1710.

(31) Hartwigsen, C.; Goedecker, S.; Hutter, J. Relativistic separable dual-space Gaussian pseudopotentials from H to Rn. *Phys. Rev. B* **1998**, *58*, 3641–3662.

(32) Perdew, J. P.; Burke, K.; Ernzerhof, M. Generalized Gradient Approximation Made Simple. *Phys. Rev. Lett.* **1996**, *77*, 3865–3868.

(33) Grimme, S.; Ehrlich, S.; Goerigk, L. Effect of the damping function in dispersion corrected density functional theory. *J. Comput. Chem.* **2011**, *32*, 1456–1465.

(34) Henkelman, G.; Jónsson, H. Improved tangent estimate in the nudged elastic band method for finding minimum energy paths and saddle points. *J. Chem. Phys.* **2000**, *113*, 9978–9985.

(35) Henkelman, G.; Uberuaga, B. P.; Jónsson, H. A climbing image nudged elastic band method for finding saddle points and minimum energy paths. *J. Chem. Phys.* **2000**, *113*, 9901–9904.

(36) Laio, A.; Parrinello, M. Escaping free-energy minima. *Proc. Natl. Acad. Sci.* **2002**, *99*, 12562–12566.

(37) Hänggi, P.; Talkner, P.; Borkovec, M. Reaction-rate theory: fifty years after Kramers. *Rev. Mod. Phys.* **1990**, *62*, 251–341.